galaxies

MDPI

Article

X-ray Observations of Planetary Nebulae since WORKPLANS I and Beyond

Martín A. Guerrero

Instituto de Astrofísica de Andalucía, IAA-CSIC, Glorieta de la Astronomía s/n, E-18008 Granada, Spain; mar@iaa.es

Received: 26 February 2020; Accepted: 13 March 2020; Published: 17 March 2020

Abstract: Planetary nebulae (PNe) were expected to be filled with hot pressurized gas driving their expansion. *ROSAT* hinted at the presence of diffuse X-ray emission from these hot bubbles and detected the first sources of hard X-ray emission from their central stars, but it was not until the advent of *Chandra* and *XMM-Newton* that we became able to study in detail their occurrence and physical properties. Here I review the progress in the X-ray observations of PNe since the first WORKshop for PLAnetary Nebulae observationS (WORKPLANS) and present the perspective for future X-ray missions with particular emphasis on *eROSITA*.

Keywords: planetary nebulae; X-ray; stellar winds; late stellar evolution

1. Introduction

Planetary nebulae (PNe) are the descendants of low- and intermediate-mass stars, as they eject their envelopes at the tip of the asymptotic giant branch (AGB) and start their evolution towards the white dwarf phase. At this time, the central star of the PN (CSPN) develops a fast (although tenuous) stellar wind that impinges and snowplows the material previously ejected during the AGB as a slow and dense stellar wind. In this interacting stellar winds (ISW) model for the formation and evolution of PNe, the fast stellar wind is shock-heated up to temperatures that depend on the CSPN terminal wind velocity as $T \sim v_\infty^2$ [1]. For typical CSPN wind velocities of $v_\infty = 500 - 4000$ km s^{-1} (e.g., [2]), shocked plasma at X-ray-emitting temperatures in excess of 10^6 K can be expected.

The very first *Chandra* observations of PNe already found hot bubbles with temperatures of a few million K confined within the inner rims of BD+30°3639 [3] and NGC 6543 [4]. This general behavior has been largely confirmed by the *Chandra* Planetary Nebula Survey (ChanPlaNS; [5,6]), a volume-limited survey of a sample of nearby ($d < 1.5$ kpc) PNe. Diffuse X-ray emission is detected only in compact ($r < 0.2$ pc) relatively young PNe with a closed-shell morphology (as suggested previously by [7]), for a detection rate ∼30%.

Chandra has also unveiled unexpected sources of hard X-ray emission (>0.5 keV) from CSPNe [8], and ChanPlaNS has confirmed the prevalence of these hard X-ray point-sources in a significant number of CSPNe [9]. Some of these hard X-ray sources can be attributed to the coronal emission from a dwarf or late-type giant companion [10], while others can be assigned to shocks in their fast winds as in OB and Wolf-Rayet stars, especially among CSPNe with powerful fast stellar winds [8]. The X-ray to bolometric luminosity ratios of the latter, $L_X/L_{bol} \sim 10^{-7}$, are indeed similar to those of single OB stars (e.g., [11]).

2. Available X-ray Observatories

ROSAT obtained pointed or serendipituous observations of 63 PNe, but only 16 were detected and most of these detections correspond to soft photospheric emission from hot CSPNe, whereas only three, namely BD+30°3639, NGC 6543, and NGC 7009 could be tentatively attributed to diffuse

hot gas [12]. Most modern X-ray observations of PNe have been obtained using the *Chandra* and *XMM-Newton* observatories, which were launched in 1999, i.e., more than 20 years ago! Still, they have been used rather than other more modern X-ray observatories such as *Swift* or *AstroSat* because of the much larger effective areas of *Chandra* and *XMM-Newton* in the energy range of interest ($\leq$1.5 keV) for PNe. Specifically, the effective area of the *Chandra* ACIS-S7 and *XMM-Newton* EPIC-pn detectors at 1.5 keV are 5–8 and 9–13 times larger, respectively, than those of *Swift* XRT ($\simeq$135 cm^2) and *AstroSat* ($\simeq$90 cm^2).

Since *Chandra* and *XMM-Newton* started operations in 1999, the number of PNe with diffuse X-ray emission and CSPNe with hard X-ray emission from grown steadily. As illustrated in the bottom panel of Figure 1, *Chandra* and *XMM-Newton* have revealed these types of X-ray emission in almost 40 PNe. The notable increase of PNe between 2010 and 2015 can be attributed to the effort of the PN community to obtain the ChanPlaNS survey, which has resulted in unprecedented progress in the understanding of the nature of point and extended sources of X-rays in PNe. The impact of all these observations has been tremendous. Almost 60 papers have been written in this topic since the launch of *Chandra* and *XMM-Newton* at a publication rate of three papers per year (top panel of Figure 1). By the end of 2019, these papers had garnered close to 1500 citations.

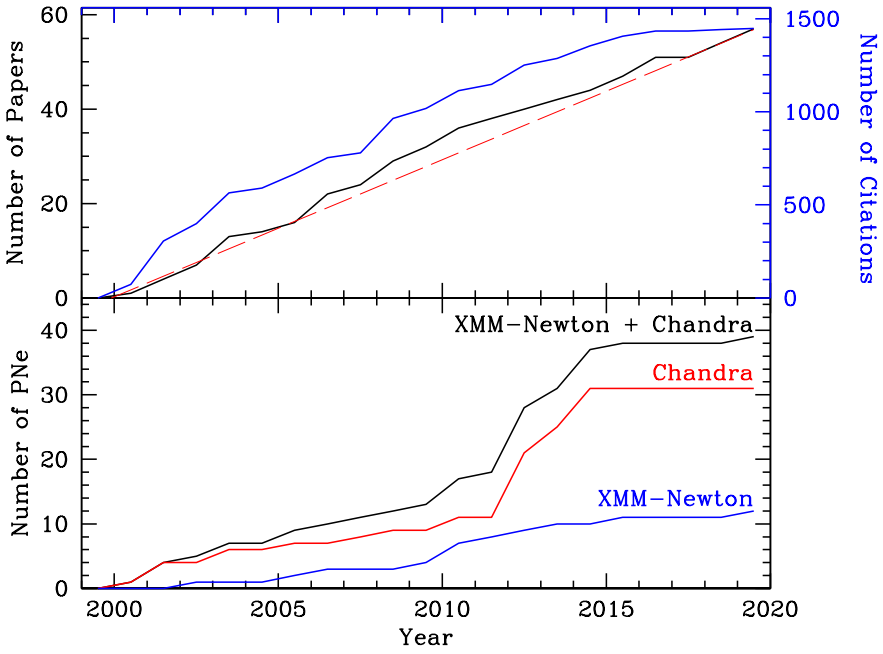

Figure 1. (bottom) Time evolution of the number of PNe detected by the *Chandra* (red) and *XMM-Newton* (blue) X-ray observatories. (top) Time evolution of the number of papers (black) and citations to these papers (blue) based on those X-ray observations (source Astronomycal Database System, ADS, at https://ui.adsabs.harvard.edu). Note that the left and right axes in this panel refer to numbers of papers and citations, respectively, as denoted by their labels and colors. The red-dashed line is a linear fit to the number of papers, implying a publication rate $\simeq$3 papers per year on the X-ray emission from PNe.

The bottom panel of Figure 1 reveals a worrisome fact. Despite its unbeatable spatial resolution, *Chandra* has not contributed to any new X-ray detection among PNe since 2014 (*XMM-Newton* has made two new discoveries since then). This can be mostly attributed to the continuous degradation of *Chandra* ACIS's sensitivity to low energy photons, which has made it more and more unlikely to

detect the soft X-ray emission from PNe with sufficient photon counts for detailed spectral analysis[1]. This is illustrated in Figure 2, showing the time evolution of the exposure time required for a *Chandra* ACIS-S observation to obtain the same number of counts for a plasma model typical of the diffuse X-ray emission in PNe. Similarly, the simulation of the *Chandra* ACIS-S count number and image of BD+30°3639 through Cycle 10 (≃2500 cnts), Cycle 15 (≃1500 cnts) and Cycle 20 (≃350 cnts) compares very poorly to those observed in Cycle 1 (≃4400 cnts, Montez, priv. communication). In this sense, the ChanPlaNS survey was very timely, using the last useful *Chandra* window to acquire imaging spectroscopic observations of PNe.

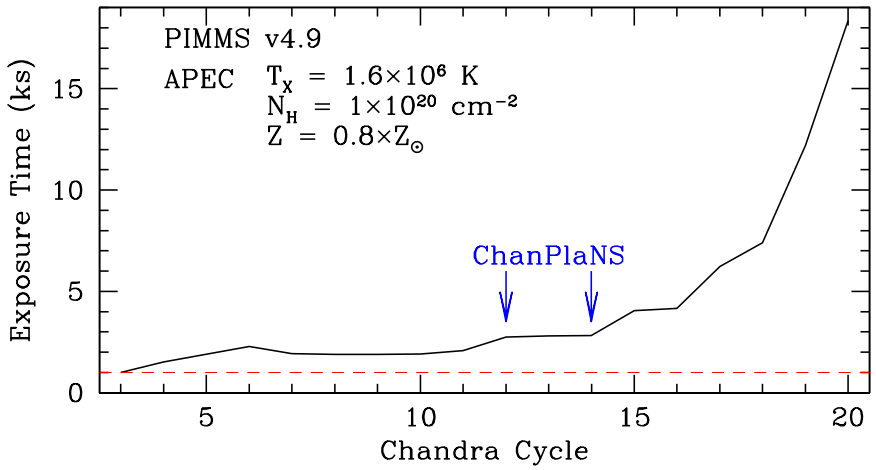

Figure 2. Time evolution of the exposure time required for a *Chandra* ACIS-S observation to obtain a given number of counts for a plasma model typical of the diffuse X-ray emission in PNe. Simulations were obtained using the *Chandra* PIMMS v4.9 simulator, which includes the most up-to-date calibrations. A plasma with a typical 1.6×10^6 K temperature, low hydrogen column density, and slightly subsolar chemical composition has been assumed.

3. Latest Results on X-ray Emission from PNe

Since the WORPLANS I meeting in December 2015, a number of new results based on X-ray observations or theoretical investigations have been reported. These can be grouped in four different categories.

3.1. Theoretical Studies

The large amount of observational data already available has allowed the refinement of our ISW models on the production of X-ray-emitting gas in PNe. Two different research lines have been pursued. The special properties of the hot bubbles produced by CSPNe with H-deficient stellar winds has been extensively investigated, with particular attention paid to the effects of heat conduction [13] and its application to the case of BD+30°3639 [14]. On the other hand, the combined effects of heat conduction and turbulent mixing have been tested using high-resolution, two-dimensional, radiation-hydrodynamical simulations [15,16]. In these detailed models, instabilities in the wind-wind interaction zone produce clumps and filaments in the swept-up shell of nebular material with notable effects in the time-dependent X-ray emission as the stellar parameters change. It is shown that the diffuse X-ray emission at early times is dominated by the contribution from the hot, shocked stellar wind, whereas the contribution from nebular gas dominates at later times. Furthermore, these models demonstrate that the X-ray temperature of a hot bubble is anti-correlated with metallicity, but its X-ray

[1] The sensitivity of *Chandra* HRC has remained basically unchanged in this time period, but the spectral capability of this instrument, which is otherwise very well suited for high-resolution imaging studies, is very limited.

luminosity increases with metallicity. The conclusions are quite robust, turbulent mixing layers are the origin of the soft X-ray emission in the majority of diffuse nebulae.

3.2. Multi-Wavelength Studies

Multi-wavelength studies combining X-ray and infrared, optical, and UV observations have provided very interesting results in the past few years. The obvious correlation between the X-ray morphology and the varying local extinction, as the soft X-ray emission from PNe is easily absorbed by even small amounts of material along the line of sight, has been confirmed through the comparison of optical and infrared images of BD+30°3639 [17] and NGC 7027 [18] with archival or new *Chandra* observations. The discovery of the mixing layer at the interface between the X-ray-emitting hot bubble and the optical photo-ionized nebular shell in NGC 6543 using *HST* STIS observations [19] is very exciting. The emission in the N V $\lambda\lambda$1239, 1243 Å lines from this interface layer has allowed for the first time not only to probe it, but to determine its spatial extent, thickness and physical properties. These are critical to assess the relative importance of heat conduction and turbulent mixing in the production of hot gas in PNe.

3.3. X-ray Variability Studies

The hard X-ray emission from the CSPN of the Eskimo Nebula has been found to be variable with a period $\simeq$6 h [20]. This X-ray emission might be attributed to accretion of material from the CSPN wind onto a white dwarf companion, and thus the observed period can be assigned either to the orbital period of the companion or to the rotation of an accretion disk around it. Time-analysis of the X-ray emission from CSPNe can be very revealing of the nature of putative companions.

3.4. New Discoveries of X-ray PNe

Only one more PN has been found to exhibit diffuse X-ray emission since the WORKPLANS I. This is the case of NGC 5189, a PN around a [WO1] CSPN whose extended X-ray emission has been discovered by *XMM-Newton* [21]. The spatial distribution and spectral properties of the X-ray emission, particularly its high carbon abundances, are consistent with a born-again scenario where a CSPN becomes carbon-rich through a very late thermal pulse (VLTP) event and then develops a fast, carbon-rich wind that generates X-ray emission. The physics of the interaction between the present fast stellar wind of the CSPN and the hydrogen-poor clumps of material ejected in the VLTP event is fascinating (see also the cases of A 30 and A 78, [22,23]).

4. The Future of X-ray Observations of PNe

In the long run, the *X-ray Imaging and Spectroscopic Mission* (*XRISM*), the *X-ray Universe Baryon Surveyor* (*HUBS*), the *Advanced Telescope for High ENergy Astrophysics* (*Athena*), and the *Lynx X-ray Observatory* (*Lynx*), with their enhanced collecting areas, high-dispersion instruments, and/or spatial resolution will play major roles in a better understanding of the production of hot gas in the interior of PNe and its role in their evolution and shaping. Meanwhile, the *eROSITA* mission will produce an X-ray map of the whole sky with unprecedented sensitivity. The final *eROSITA* All Sky Survey (eRASS) is expected to have a sensitivity in the range from 1×10^{-14} down to 3×10^{-17} erg cm^{-2} s^{-1}, depending on the final exposure time of a particular position on the sky.

We have convolved the expected sensitivity map of the final eRASS with the position of all known PNe to determine their exposure times and X-ray sensitivity. The expected distributions of exposure times and sensitivities for the whole sample of known PNe are shown in Figure 3. It reveals that $\simeq$200 PNe will be observed with exposure times greater than 20 ks. As the seven X-ray telescopes of *eROSITA* have a total effective area above that of *XMM-Newton* EPIC-pn, almost 500 PNe will have observations as sensitive, $\leq2\times10^{-15}$ erg cm^{-2} s^{-1}, as those of PNe in the ChanPlaNS survey. Obviously this will produce a major improvement in our statistics of the presence of X-ray emission in PNe.

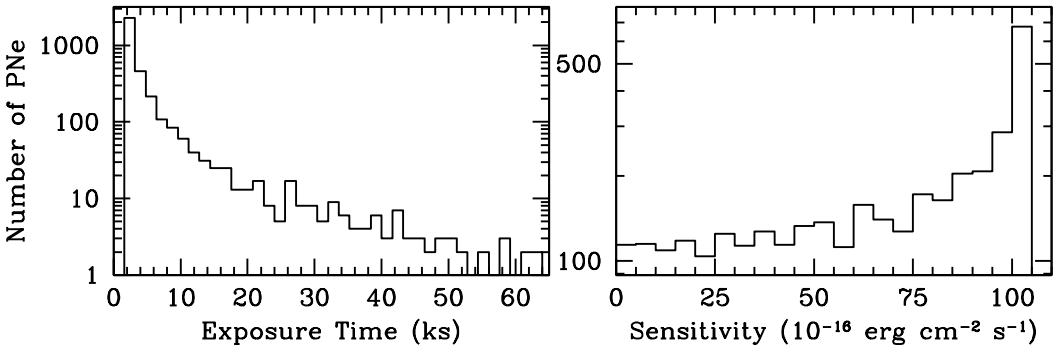

Figure 3. Distribution of exposure time (left) and sensitivity (rigth) for PNe expected in the final eRASS map of the whole sky. Most PNe will be located in areas of the eRASS with total exposure times shorter than 20 ks, but a significant number of them, $\simeq$200, will have longer exposure times. Accordingly, a significant number of PNe, those with long exposure times in the final eRASS, will have observations with sensitivities adequate to detect X-ray fluxes smaller than $\simeq 2\times10^{-15}$ erg cm^{-2} s^{-1}.

5. Conclusions

Since the advent of the modern X-ray observatories *Chandra* and *XMM-Newton*, the number of PNe with diffuse X-ray emission and CSPNe with hard X-ray emission have grown steadily. The large number and quality of these X-ray data sets of PNe has resulted in major advances in a research field for which sensitive observations basically did not exist before 1999. Over 60 papers have been generated based on these observations since 1999, garnering almost 1500 citations.

This publication rate has remained since the last WORKPLANS meeting in December 2015, but the emphasis of the studies has changed significantly. In this time period, notable advances in theoretical analyses have been made and multi-wavelength and time-domain studies are gaining momentum, while the discoveries of new cases for X-ray emission from PNe or their CSPNe has slowed nearly to a halt, mostly due to the dramatic decrease of sensitivity to soft X-ray photons of *Chandra* ACIS.

In the near future, *eROSITA* can make a major contribution to our understanding of the production of hot gas in PNe and its effects in their evolution and shaping. Hundreds of PNe can be expected to be observed with sensitivities similar to many of the currently available observations carried out by *Chandra* and *XMM-Newton* in the last two decades.

Funding: This research was funded by the Spanish Ministerio de Ciencia, Innovación y Universidades grant number PGC2018-102184-B-I00 co-funded by FEDER funds.

Acknowledgments: The author acknowledges the scientific discussions with Joel H. Kastner, Rodolfo Montez, Quentin Parker, and Jesús A. Toalá, which helped him assess the impact of *eROSITA* and its eRASS for the research of X-ray emission from PNe. Four anonymous referees are also acknowledged for their useful comments and suggestions to improve this manuscript.

Conflicts of Interest: The author declare no conflict of interest.

References

1. Dyson, J.E.; Williams, D.A. *The Physics of the Interstellar Medium*, 2nd ed.; Institute of Physics Publishing: Bristol, UK, 1997.
2. Guerrero, M.A.; De Marco, O. Analysis of far-UV data of central stars of planetary nebulae: Occurrence and variability of stellar winds. *Astron. Astrophys.* **2013**, *553*, A126. [CrossRef]
3. Kastner, J.H.; Soker, N.; Vrtilek, S.D.; Dgani, R. *Chandra* X-Ray Observatory Detection of Extended X-Ray Emission from the Planetary Nebula BD+30°3639. *Astrophys. J. Lett.* **2000**, *545*, L57. [CrossRef]
4. Chu, Y.-H.; Guerrero, M.A.; Gruendl, R.A.; Williams, R.M.; Kaler, J.B. Chandra Reveals the X-Ray Glint in the Cat's Eye. *Astrophys. J. Lett.* **2001**, *553*, L69. [CrossRef]
5. Freeman, M.; Montez, R.; Kastner, J.H. The *Chandra* Planetary Nebula Survey (ChanPlaNS). II. X-Ray Emission from Compact Planetary Nebulae. *Astrophys. J.* **2014**, *794*, 99. [CrossRef]

6. Kastner, J.H.; Montez, R.; Balick, B.; Frew, D.J.; Miszalski, B.; Sahai, R.; Blackman, E.; Chu, Y.-H.; De Marco, O.; Frank, A. The *Chandra* X-Ray Survey of Planetary Nebulae (ChanPlaNS): Probing Binarity, Magnetic Fields, and Wind Collisions. *Astrophys. J.* **2012**, *144*, 58.
7. Ruiz, N.; Guerrero, M.A.; Chu, Y.-H.; Gruendl, R.A. Physical Structure of the Planetary Nebula NGC 3242 from the Hot Bubble to the Nebular Envelope. *Astrophys. J.* **2011**, *142*, 91. [CrossRef]
8. Guerrero, M.A.; Chu, Y.-H.; Gruendl, R.A.; Williams, R.M.; Kaler, J.B. The Enigmatic X-Ray Point Sources at the Central Stars of NGC 6543 and NGC 7293. *Astrophys. J. Lett.* **2001**, *553*, L55. [CrossRef]
9. Montez, R.; Kastner, J.H.; Balick, B.; Behar, E.; Blackman, E.; Bujarrabal, V.; Chu, Y.-H.; Corradi, R.L.M.; De Marco, O.; Frank, A.; et al. The Chandra Planetary Nebula Survey (ChanPlaNS). III. X-Ray Emission from the Central Stars of Planetary Nebulae. *Astrophys. J.* **2015**, *800*, 8. [CrossRef]
10. Montez, R.; De Marco, O.; Kastner, J.H.; Chu, Y.-H. X-ray Emission from the Binary Central Stars of the Planetary Nebulae HFG 1, DS 1, and LoTr 5. *Astrophys. J.* **2010**, *721*, 1820. [CrossRef]
11. Nebot Gómez-Morán, A.; Oskinova, L.M. The X-ray catalog of spectroscopically identified Galactic O stars. Investigating the dependence of X-ray luminosity on stellar and wind parameters. *Astron. Astrophys.* **2018**, *620*, A89. [CrossRef]
12. Guerrero, M.A.; Chu, Y.-H.; Gruendl, R.A. *ROSAT* Observations of X-Ray Emission from Planetary Nebulae. *ApJS* **2000**, *129*, 295. [CrossRef]
13. Sandin, C.; Steffen, M.; Schönberner, D.; Rühling, U. Hot bubbles of planetary nebulae with hydrogen-deficient winds. I. Heat conduction in a chemically stratified plasma. *Astron. Astrophys.* **2016**, *586*, A57. [CrossRef]
14. Heller, R.; Jacob, R.; Schönberner, D.; Steffen, M. Hot bubbles of planetary nebulae with hydrogen-deficient winds. II. Analytical approximations with application to BD+30°3639. *Astron. Astrophys.* **2018**, *620*, A98. [CrossRef]
15. Toalá, J.A.; Arthur, S.J. Formation and X-ray emission from hot bubbles in planetary nebulae—II. Hot bubble X-ray emission. *MNRAS* **2016**, *463*, 4438–4458. [CrossRef]
16. Toalá, J.A.; Arthur, S.J. On the X-ray temperature of hot gas in diffuse nebulae. *MNRAS* **2018**, *478*, 1218–1230.
17. Freeman, M.J.; Kastner, J.H. A Multi-wavelength 3D Model of BD+30°3639. *ApJS* **2016**, *226*, 15. [CrossRef]
18. Montez, R.; Kastner, J.H. Dissecting the X-Ray Emission in the Young Planetary Nebula NGC 7027. *Astrophys. J.* **2018**, *861*, 45. [CrossRef]
19. Fang, X.; Guerrero, M.A.; Toalá, J.A.; Chu, Y.-H.; Gruendl, R.A. HST STIS Observations of the Mixing Layer in the Cat's Eye Nebula. *Astrophys. J. Lett.* **2016**, *822*, L19. [CrossRef]
20. Guerrero, M.A.; Toalá, J.A.; Chu, Y.-H. Variable Hard X-Ray Emission from the Central Star of the Eskimo Nebula. *Astrophys. J.* **2019**, *884*, 134. [CrossRef]
21. Toalá, J.A.; Montez, R.; Karovska, M. A Carbon-rich Hot Bubble in the Planetary Nebula NGC 5189. *Astrophys. J.* **2019**, *886*, 30.
22. Guerrero, M.A.; Ruiz, N.; Hamann, W.-R.; Chu, Y.-H.; Todt, H.; Schönberner, D.; Oskinova, L.; Gruendl, R.A.; Steffen, M.; Blair, W.P.; et al. Rebirth of X-Ray Emission from the Born-again Planetary Nebula A 30. *Astrophys. J.* **2012**, *755*, 129. [CrossRef]
23. Toalá, J.A.; Guerrero, M.A.; Todt, H.; Hamann, W.-R.; Chu, Y.-H.; Gruendl, R.A.; Schönberner, D.; Oskinova, L.M.; Marquez-Lugo, R.A.; Fang, X.; et al. The Born-again Planetary Nebula A 78: An X-Ray Twin of A 30. *Astrophys. J.* **2015**, *799*, 67. [CrossRef]